Gas Solubility of Carbon Dioxide and of Oxygen in Cyclohexanol by Experiment and Molecular Simulation

T. Merker[a], J. Vrabec[b], H. Hasse[a,*]

[a] *Laboratory of Engineering Thermodynamics, University of Kaiserslautern, 67663 Kaiserslautern, Germany*
[b] *Thermodynamics and Energy Technology, University of Paderborn, 33098 Paderborn, Germany*

Abstract

Henry's law constant data of carbon dioxide and of oxygen in liquid cyclohexanol are determined at temperatures between 303 and 392 K by means of a precise experimental high-pressure view-cell technique with a synthetic method. Furthermore, molecular simulations are carried out with a molecular mixture model, based on the modified Lorentz-Berthelot combination rule that contains one binary interaction parameter which is adjusted to one experimental Henry's law constant for each binary mixture. The molecular model yields good results for the Henry's law constant over the entire temperature range.

Keywords: cyclohexanol, carbon dioxide, oxygen, experiment, gas solubility, Henry's law constant, molecular simulation

1. Introduction

The oxidation of cyclohexane to cyclohexanol and cyclohexanone is an important industrial reaction and a key step in the nylon production chain. Usually, the reaction is carried out by contacting air with liquid cyclohexane from 398 to 438 K and from 0.8 to 1.5 MPa [1]. Due to oxidative side

*Corresponding author: Hans Hasse
Technische Universität Kaiserslautern, Lehrstuhl für Thermodynamik, Erwin-Schrödinger-Straße 44, 67663 Kaiserslautern, Germany, *phone* +49 631 205 3464, *fax* +49 631 205 3835
Email address: hans.hasse@mv.uni-kl.de (H. Hasse)
URL: thermo.mv.uni-kl.de (H. Hasse)

reactions, the process must be carried out at a low conversion rate of around 10 % in order to allow for an acceptable selectivity of about 85 % towards cyclohexanone and cyclohexanol [1].

Alternative routes are being studied for this process step. One option is to use novel octahedral molecular sieves (OMS) for the heterogeneously catalyzed selective oxidation of cyclohexane [2]. Liquids expanded by supercritical carbon dioxide can be used to enhance the mobility of both the reactants and the products, leading to a higher conversion rate and a good yield [3]. Furthermore, the use of carbon dioxide expanded reaction media may have additional benefits, like better heat and mass transfer. A detailed review on the advantages of using supercritical carbon dioxide in such processes was recently published by Seki and Baiker [4]. For a rational planning of catalytic experiments and process design, especially at elevated pressures, reliable thermodynamic data are needed. The present study covers two important binary subsystems of the reaction mixture, namely carbon dioxide + cyclohexanol and oxygen + cyclohexanol.

For the gas solubility of carbon dioxide in cyclohexanol Begley et al. [5], Chen and Lee [6], Laugier and Richon [7] as well as Esmelindro et al. [8] published experimental data between 303 and 453.2 K. Esmelindro et al. [8] found a complex phase behavior for this system, including two-phase vapor-liquid equilibria (VLE), liquid-liquid equilibria (LLE) and three-phase vapor-liquid-liquid equilibria (VLLE).

Only little work has been done on the gas solubility of oxygen in cyclohexanol. Cauquil [9] and Naumenko [10] measured one Henry's law constant at 299.15 and 298.15 K, respectively. However, these data are very contradictory, with a Henry's law constant of 121 MPa by Cauquil [9] and 212 MPa by Naumenko [10]. With this poor experimental database, no quantitatively sound conclusion about the gas solubility of oxygen in cyclohexanol can be made.

In the present work, new experimental data for the gas solubility of carbon dioxide in cyclohexanol and of oxygen in cyclohexanol are reported. Therefore, the Henry's law constant was determined and the results are compared to experimental data from the literature. Additionally, molecular simulations were performed, where one state-independent binary interaction parameter was adjusted to one experimental Henry's law constant from the present work. The results are compared with the Peng-Robinson equation of state (EOS) [11].

2. Experimental Apparatus and Method

A synthetic method was applied for the present gas solubility experiments. The employed apparatus is the same as in previous works of our laboratory [12, 13, 14, 15, 16, 17]. Figure 1 shows a schematic of the gas solubility apparatus. The experiment determines the pressure that is required to dissolve a precisely known amount of a gaseous component in a precisely known amount of a solvent. The central element of the apparatus is a thermostatted cylindrical, high-pressure view cell (volume about 30 cm^3) with two sapphire windows on each end.

In an experiment, the cell is first evacuated. Then, the gaseous component is charged into the cell from a gas cylinder. The mass of this gas is determined volumetrically from the known volume of the cell and readings for temperature and pressure by applying an EOS for the pure gas (by Span and Wagner [18] for carbon dioxide and by Schmidt and Wagner [19] for oxygen). Then, the solvent is added into the cell by means of a high-pressure spindle press until the gas is completely dissolved in the liquid. After equilibration, very small amounts of the solvent are withdrawn step by step until the first very small stable gas bubbles appear. The pressure at which the degassing starts is the solubility pressure. The mass of the solvent in the cell is calculated from the volume displacement of the calibrated spindle press and the solvent density. The solvent density is determined by separate measurements with a vibrating tube densimeter (model DMA 4500M, Anton Paar).

Two calibrated platinum resistance thermometers in the thermostatted jacket of the view cell were used to determine the temperature. The solubility pressure was measured with a precise pressure transducer (WIKA, full scale 10 MPa) in connection with a mercury barometer (Lambrecht). All pressure transducers were calibrated against a high-precision pressure balance (Desgranges & Huot).

The maximum uncertainty of the solubility pressure measurements is due to the intrinsic uncertainty of the pressure transducers (0.1% of the transducer's full scale, i.e. 0.01 MPa here) and an additional contribution of about 0.01 MPa from a small temperature drift inside the isolated (high-pressure) tubes filled with the solvent that connect the view cell with the pressure transducer. The uncertainty of the temperature measurement is ± 0.1 K.

Oxygen (4.5, volume fraction 99.995%) and carbon dioxide (4.5, volume fraction 99.995%) were purchased from Messer Griesheim, Germany. Cyclohexanol (purity $\geq$ 99.0%) was purchased from Sigma-Aldrich, Germany and

degassed in our laboratory under vacuum.

3. Henry's Law Constant

3.1. Experiment

The mole fraction based Henry's law constant of carbon dioxide or oxygen (solute i) in cyclohexanol $H_i(T)$ (at the vapor pressure of pure cyclohexanol p_c^s) was determined from the present experimental data using an extrapolation procedure at constant temperature

$$H_i(T) = \lim_{p \to p_c^s} \left[\frac{f_i(T, p, y_i)}{x_i} \right], \tag{1}$$

where

$$f_i(T, p, y_i) = p y_i \varphi_i(T, p, y_i). \tag{2}$$

The fugacity of the gaseous component i is f_i and its fugacity coefficient is φ_i. x_i and y_i are the mole fractions of the gaseous component i in the liquid and the vapor, respectively.

The vapor pressure of pure cyclohexanol p_c^s was calculated from a DIPPR correlation [20]. As the vapor pressure of cyclohexanol is low, it was assumed that the vapor consists only of the solute gas, i.e. $y_i = 1$. The vapor phase fugacity coefficient φ_i of carbon dioxide and oxygen was calculated with the EOS by Span and Wagner [18] and the EOS by Schmidt and Wagner [19], respectively.

3.2. Molecular Simulation

The Henry's law constant H_i is related to the residual chemical potential of the solute i at infinite dilution in the solvent μ_i^∞ [21] by

$$H_i(T) = \rho_c^s k_B T \exp(\mu_i^\infty / (k_B T)), \tag{3}$$

where k_B is Boltzmann's constant and ρ_c^s is the number density of cyclohexanol in its saturated liquid state. For a specified temperature, H_i can be obtained by a single molecular simulation run. Sampling the saturated liquid state point of the pure solvent, simply the residual chemical potential of the solute μ_i^∞ has to be determined. Due to the hydrogen bonding interaction of cyclohexanol, Widom's insertion method [22] yields results with large statistical uncertainties, especially at lower temperatures. Therefore, gradual

insertion [23] was used here to determine the residual chemical potential at infinite solution. One gas molecule was added to a sufficiently large molecular system containing $N \approx 1000$ cyclohexanol molecules. For validation, Henry's law constant data determined by Widom's insertion method and by gradual insertion were compared at temperatures where Widoms's insertion method yields reliable results. Both methods agree within their statistical errors, cf. Figure 2. Technical simulation details are given in the appendix.

All pure substance molecular models were taken from preceding work of our group. Carbon dioxide [24] and oxygen [25] were described by three and two Lennard-Jones (LJ) sites, respectively, and one point quadrupole. The cyclohexanol model [26] consists of seven LJ sites and three point charges, to cover electrostatics and hydrogen bonding.

To describe mixtures on the basis of pairwise additive potentials, molecular modeling reduces to modeling the interactions between unlike molecules. The unlike polar interactions were treated in a straightforward manner following the laws of electrostatics without binary parameters. For the unlike LJ interactions, the modified Lorentz-Berthelot combination rule with one state-independent binary parameter ξ was used [27]

$$\sigma_{\mathrm{AB}} = (\sigma_{\mathrm{A}} + \sigma_{\mathrm{B}})/2, \tag{4}$$

and

$$\epsilon_{\mathrm{AB}} = \xi\sqrt{\epsilon_{\mathrm{A}}\epsilon_{\mathrm{B}}}. \tag{5}$$

The binary parameter ξ was adjusted here to a single experimental Henry's law constant per binary system. Table 1 contains the temperature and the experimental Henry's law constant which was used for the adjustment as well as the resulting binary parameter ξ and the respective simulation results.

4. Results and Discussion

4.1. Gas Solubility

The solubility of carbon dioxide in cyclohexanol was measured at T= 303.8, 313.6, 352.9 and 392 K for total pressures of up to 7.7 MPa, cf. Table 2. Present experimental results are compared to experimental data by Chen and Lee [6] and to the Peng-Robinson EOS [11] in Figure 3. Note that the isotherm 313.6 K is not shown for better visibility of the remaining data. As depicted in Figure 3, a typical physical gas solubility behavior is observed. For all amounts of the gas in the liquid, the solubility pressure increases

almost linearly with increasing amount of dissolved gas. Also, the solubility of carbon dioxide decreases with rising temperature, which is typical for a well soluble gas. Between 303.8 and 352.9 K, a much stronger decrease of the solubility can be seen than between 352.9 and 392 K. VLLE, as reported by Esmelindro et al. [8] for 313.5 K, were not observed for the measured carbon dioxide concentrations here. The present gas solubility results and those of Chen and Lee [6] are in good agreement. The Peng-Robinson EOS [11] overpredicts the gas solubility pressure for higher temperatures. Also, for the lower temperatures, the Peng-Robinson EOS [11] was not capable to calculate VLE for carbon dioxide mole fractions above around 0.29 mol/mol. This indicates the occurence of a VLLE as reported by Esmelindro et al. [8]. The Peng-Robinson EOS [11] with one adjustable parameter can not quantitatively describe the gas solubility for this system.

The solubility of oxygen in cyclohexanol is presented in Table 2 and in Figure 3 at T= 303.8, 313.6 and 352.9 K and for pressures of up to 10 MPa. The present experimental results are compared to the Peng-Robinson EOS [11]. The isotherm 313.6 K was again excluded from the Figure for visibility reasons. As for the gas solubility of carbon dioxide, a typical physical gas solubility behavior was observed. With rising temperature, the solubility of oxygen increases only slightly as often reported for poorly soluble gases.

4.2. Henry's Law Constant

In Figure 4, the ratio f_i/x_i is presented that was determined from the isothermal experimental data for the systems (carbon dioxide + cyclohexanol) and (oxygen + cyclohexanol). The isotherm 313.6 K was again excluded for better visibility. The extrapolation was done by linear regression. The resulting numerical values for the Henry's law constant of carbon dioxide and of oxygen in cyclohexanol are given in Table 3. The Henry's law constant is plotted in Figure 2 as a function of temperature.

The present experimental Henry's law constant data for carbon dioxide in cyclohexanol are compared to molecular simulation results from the present work as well as to experimental data by Begley et al. [5] and by Chen and Lee [6] in Figure 2. Due to the decreasing gas solubility, the Henry's law constant rises with rising temperature. The present experimental data are in very good agreement both with the data by Begley et al. [5] as well as by Chen and Lee [6]. Molecular simulations are in a very good agreement for lower temperatures, at higher temperatures, the Henry's law constant was

overpredicted with an maximum deviation of around 15 % at 392 K compared to the present experimental results.

The present experimental Henry's law constant data for oxygen in cyclohexanol are presented in Figure 2 together with the experimental data by Cauquil [9] and by Naumenko [10] as well as with the present molecular simulation results. According to the observations for the gas solubility, the Henry's law constant decreases with rising temperature. The relatively large error bars of the present experiments are due to the very small mole fraction of oxygen in liquid cyclohexanol, cf. Figure 3. The present experimental data are in good agreement with the data by Naumenko [10], while Cauquil [9] reported a much lower Henry's law constant. Molecular simulation is in good agreement with the present experimental data.

In addition to the Henry's law constant, the enthalpy of solution was determined from the temperature dependence of the Henry's law constant [28] from experiment and molecular simulation. For carbon dioxide, the enthalpy of solution is -5.1 (± 0.1) kJ/mol (experiment) and -6 (± 0.4) kJ/mol (simulation), respectively. The difference between experiment and simulation is due to the overprediction of the simulations at higher temperatures leading to a higher inclination and thus a more negative enthalpy of solution. For oxygen the, enthalpy of solution for experiment and simulation is 2.5 (± 0.3) kJ/mol and 2.25 (± 0.05) kJ/mol, respectively. Here, the data agrees within their uncertainties.

5. Conclusions

Experimental results were presented for the solubility of the single components carbon dioxide and oxygen in pure liquid cyclohexanol. From these data, the Henry's law constant of carbon dioxide and of oxygen in cyclohexanol was determined.

The Henry's law constant of carbon dioxide in cyclohexanol rises with increasing temperature. The present experimental results are in good agreement with the experimental data from the literature. Molecular simulation overpredicts the Henry's law constant at higher temperatures for this system.

The ambiguity of literature data for the Henry's law constant of oxygen in cyclohexanol was resolved. The experimental data point by Naumenko was confirmed by the present experiments. The Henry's law constant decreases with rising temperature and molecular simulation is in good agreement with the present experimental results.

Additionally, the enthalpy of solution was determined via experiment and simulation. For carbon dioxide, the simulations showed a more negative enthalpy of solution then the experiment. For oxygen, simulation and experiment agree within their uncertainties.

6. Appendix: Simulation Details

Gradual insertion was applied in conjunction with Monte Carlo simulations in the NpT ensemble using one solute molecule and 999 cyclohexanol molecules. Starting from a face centred cubic lattice, 35 000 Monte Carlo cycles were performed for equilibration with the first 10 000 cycles in the canonical (NVT) ensemble and 200 000 cycles for production. Each cycle contained 1000 displacement moves, 1000 rotation moves and 1 volume move. Every 50 cycles, 10 000 fluctuating state change moves, 10 000 fluctuating particle translation/rotation moves and 50 000 biased particle translation/rotation moves were performed to determine the chemical potential. The maximum displacements for translation, rotation and volume were adjusted to yield acceptance rates of 50 %.

Widom's method was applied in conjunction with molecular dynamics simulations in the NpT ensemble using isokinetic velocity scaling [29] and Anderson's barostat [30]. There, the number of molecules was 1372 and the time step was 1 fs. The initial configuration was a face centred cubic lattice, the fluid was equilibrated over 150 000 time steps with the first 50 000 time steps in the canonical (NVT) ensemble. The production run went over 400 000 time steps with a piston mass of 10^9 kg/m^4. Up to 5 000 test molecules were inserted every production time step.

The cut-off radius was set to at least 15 Å and a center of mass cut-off scheme was employed. Lennard-Jones long-range interactions beyond the cut-off radius were corrected as proposed by Lustig [31]. The electrostatic interactions were approximated by a resulting molecular dipole and corrected with the reaction field method [29]. Statistical uncertainties of the simulated values were estimated by a block averaging method [32].

All calculations were performed with the molecular simulation tool $ms2$ [33].

The adjustable binary parameter k_{ij} of the following mixing rules

$$a_{ij} = \sqrt{a_{ii} a_{jj}}(1 - k_{ij}). \tag{6}$$

and

$$b_{ij} = (b_{ii} + b_{jj})/2, \tag{7}$$

where a_{ij} and b_{ij} are the cross parameters of the one-fluid mixing rule of van der Waals used in the Peng-Robinson EOS [11].

Acknowledgement

The authors gratefully acknowledge financial support by Deutsche Forschungsgemeinschaft, Collaborative Research Centre SFB 706 "Selective Catalytic Oxidations Using Molecular Oxygen". The presented research was conducted under the auspices of the Boltzmann-Zuse Society of Computational Molecular Engineering (BZS). The simulations were performed on the national super computer NEC SX-8 at the High Performance Computing Centre Stuttgart (HLRS) under the grant MMHBF and on the HP XC4000 super computer at the Steinbuch Centre for Computing under the grant LAMO.

References

[1] K. Weissermel, H.-J. Arpe, Industrial Organic Chemistry, VCH Press, Weinheim, 1997.

[2] F. Schurz, J. M. Bauchert, T. Merker, T. Schleid, H. Hasse, R. Gläser, App. Catal. A 355 (2009) 42–49.

[3] W. Leitner, Acc. Chem. Res. 35 (2002) 746–756.

[4] T. Seki, A. Baiker, Chem. Rev. 109 (2009) 2409–2454.

[5] J. W. Begley, H. J. R. Maget, B. Williams, J. Chem. Eng. Data. 10 (1965) 4–8.

[6] J.-T. Chen, M.-J. Lee, J. Chem. Eng. Data. 41 (1996) 339–343.

[7] S. Laugier, D. Richon, J. Chem. Eng. Data 42 (1997) 155–159.

[8] M. C. Esmelindro, O. A. C. Antunes, E. Franceschi, G. R. Borges, M. L. Corazza, J. V. Oliveira, W. Linhares, C. Dariva, J. Chem. Eng. Data 53 (2008) 2050–2055.

[9] G. Cauquil, J. Chim. Phys. Phys.-Chim. Biol. 24 (1926) 53–55.

[10] N. K. Naumenko, Leningrad, PhD thesis, 1970.

[11] D. Y. Peng, D. B. Robinson, Ind. Chem. Eng. Fundam. 15 (1976) 59–64.

[12] J. Xia, A. Pérez-Salado Kamps, G. Maurer, J. Chem Eng. Data 49 (2004) 1756–1759.

[13] B. Rumpf, Untersuchungen zur Löslichkeit reagierender Gase in Wasser und salzhaltigen wässrigen Lösungen, University of Kaiserslautern, PhD thesis, 1992.

[14] B. Rumpf, G. Maurer, Fluid Phase Equilib. 81 (1992) 241–260.

[15] B. Rumpf, G. Maurer, Ber. Bunsen-Ges. Phys. Chem. 97 (1993) 85–97.

[16] A. Pérez-Salado Kamps, E. Meyer, B. Rumpf, G. Maurer, J. Chem. Eng. Data 52 (2007) 817–832.

[17] T. Merker, N. Franke, R. Gläser, T. Schleid, H. Hasse, J. Chem. Eng. Data 56 (2011) 2477–2481.

[18] R. Span, W. Wagner, J. Phys. Chem. Ref. Data 25 (1996) 1509–1596.

[19] R. Schmidt, W. Wagner, Fluid Phase Equilib. 19 (1985) 175–200.

[20] R. L. Rowley, W. V. Wilding, J. L. Oscarson, Y. Yang, N. A. Zundel, T. E. Daubert, R. P. Danner, DIPPR® Data Compilation of Pure Compound Properties, Design Institute for Physical Properties, AIChE, New York, 2006.

[21] K. S. Shing, K. E. Gubbins, K. Lucas, Mol. Phys. 65 (1988) 1235–1252.

[22] B. Widom, J. Chem. Phys. 39 (1963) 2808–2812.

[23] J. Vrabec, M. Kettler, H. Hasse, Chem. Phys. Lett. 356 (2002) 431–436.

[24] T. Merker, C. Engin, J. Vrabec, H. Hasse, J. Chem. Phys. 132 (2010) 234512.

[25] J. Stoll, Molecular Models for the Prediction of Thermophysical Properties of Pure Fluids and Mixtures, Reihe 3, VDI-Verlag, Düsseldorf, 2005.

[26] T. Merker, J. Vrabec, H. Hasse, Soft Materials 10 (2012) 3–25.

[27] T. Schnabel, J. Vrabec, H. Hasse, J. Mol. Liq. 135 (2007) 170–178.

[28] A. E. Sherwood, J. M. Prausnits, AIChE 8 (1962) 419–521.

[29] M. P. Allen, D. J. Tildesley, Computer simulations of liquids, Clarendon Press, Oxford, 1987.

[30] H. C. Anderson, J. Chem. Phys. 72 (1980) 2384–2393.

[31] R. Lustig, Mol. Sim. 37 (2011) 457–465.

[32] H. Flyvbjerg, H. G. Petersen, J. Chem. Phys. 91 (1989) 461–466.

[33] S. Deublein, B. Eckl, J. Stoll, S. V. Lishchuk, G. Guevara-Carrion, C. W. Glass, T. Merker, M. Bernreuther, H. Hasse, J. Vrabec, Comp. Phys. Commun. 182 (2011) 2350–2367.

List of Tables

1 Binary interaction parameter ξ, Henry's law constant used for the adjustment, simulation results with adjusted ξ and binary parameter k_{ij} of the Peng-Robinson EOS. The number in parentheses indicate the uncertainty in the last digit. A definition of the binary parameter k_{ij} is given in the appendix. 13

2 Experimental gas solubility of carbon dioxide (1) and of oxygen (2) in liquid cyclohexanol (3). The number in parentheses indicates the uncertainty in the last digit. 14

3 Henry's law constant of carbon dioxide and of oxygen in cyclohexanol from experiment and molecular simulation. The numbers in parentheses indicate the uncertainty in the last digits. 15

Table 1: Binary interaction parameter ξ, Henry's law constant used for the adjustment, simulation results with adjusted ξ and binary parameter k_{ij} of the Peng-Robinson EOS. The number in parentheses indicate the uncertainty in the last digit. A definition of the binary parameter k_{ij} is given in the appendix.

Mixture (i + 3)	ξ	T	H_i^{exp}	H_i^{sim}	k_{ij}
		K	MPa	MPa	
Carbon dioxide + Cyclohexanol	0.918	313.6	27.1 (7)	27.8(8)	0.189
Oxygen + Cyclohexanol	0.91	313.6	201 (11)	194.1(5)	0.322

Table 2: Experimental gas solubility of carbon dioxide (1) and of oxygen (2) in liquid cyclohexanol (3). The number in parentheses indicates the uncertainty in the last digit.

$T = 303.8$ K		$T = 313.6$ K		$T = 352.9$ K		$T = 392$ K	
Carbon dioxide (1) + Cyclohexanol (3)							
x_1	p	x_1	p	x_1	p	x_1	p
mol mol^{-1}	MPa	mol mol^{-1}	MPa	mol mol^{-1}	MPa	mol mol^{-1}	MPa
0.049(1)	1.09	0.049(1)	1.26	0.043(1)	1.40	0.041(1)	1.48
0.081(2)	1.79	0.078(1)	2.00	0.064(1)	2.00	0.046(1)	1.65
0.115(2)	2.52	0.092(2)	2.28	0.082(2)	2.58	0.059(1)	2.09
0.145(3)	3.17	0.115(2)	2.78	0.104(2)	3.22	0.060(1)	2.13
0.170(4)	3.69	0.141(2)	3.35	0.124(2)	3.77	0.078(1)	2.76
0.197(3)	4.19	0.166(3)	3.91	0.144(2)	4.38	0.096(2)	3.36
0.225(3)	4.69	0.189(3)	4.44	0.164(2)	4.98	0.115(2)	3.96
0.263(6)	5.35	0.219(3)	5.05	0.186(3)	5.65	0.132(2)	4.60
0.297(5)	5.91	0.245(4)	5.59	0.206(3)	6.25	0.150(2)	5.17
0.347(5)	6.85	0.277(5)	6.26	0.229(3)	6.92	0.171(2)	5.90
		0.308(6)	6.87	0.244(4)	7.35	0.187(3)	6.45
						0.206(4)	7.07
						0.223(4)	7.69
Oxygen (2) + Cyclohexanol (3)							
x_2	p	x_2	p	x_2	p		
mol mol^{-1}	MPa	mol mol^{-1}	MPa	mol mol^{-1}	MPa		
0.013(1)	2.69	0.016(1)	2.77	0.012(1)	2.17		
0.022(1)	4.47	0.022(1)	4.49	0.019(1)	3.48		
0.025(1)	5.28	0.026(1)	5.32	0.025(1)	4.57		
0.034(1)	7.27	0.029(1)	6.07	0.027(1)	4.98		
0.038(1)	8.21	0.033(1)	7.07	0.032(1)	5.89		
0.046(1)	10.08	0.037(1)	7.89	0.034(1)	6.34		

Table 3: Henry's law constant of carbon dioxide and of oxygen in cyclohexanol from experiment and molecular simulation. The numbers in parentheses indicate the uncertainty in the last digits.

	Carbon Dioxide		Oxygen	
T	$H_{\mathrm{CO2}}^{\mathrm{exp}}$	$H_{\mathrm{CO2}}^{\mathrm{sim}}$	$H_{\mathrm{O2}}^{\mathrm{exp}}$	$H_{\mathrm{O2}}^{\mathrm{sim}}$
K	MPa	MPa	MPa	MPa
303.8	22.8(5)	24 (1)	197(21)	199.6(7)
313.6	27.1(7)	27.8(8)	201(11)	194.1(5)
323.15		31.0(8)		192.2(5)
333.15		33.5(6)		196.6(4)
343.15		35.8(6)		187.2(4)
352.9	33.2(8)	36.6(5)	174(10)	179.6(4)
363.15		38.7(5)		176.8(3)
373.15		40.2(4)		172.6(2)
383.15		42.3(3)		167.8(2)
392	37.0(9)	42.4(3)		161.8(2)

List of Figures

1 Schematic of the gas solubility apparatus. 17

2 Henry's law constant $H_{1,3}$ of carbon dioxide (1) in cyclohexanol (3): • present experimental data ; + experimental data by Begley et al [5]; × experimental data by Chen and Lee [6]; ○ present simulation data. Henry's law constant $H_{2,3}$ of oxygen (2) in cyclohexanol (3): ■ present experimental data; ▼ experimental data by Naumenko [10]; ▲ experimental data by Cauquil [9]; □ present simulation data (gradual insertion); △ present simulation data (Widom). The error bars of the present data are not shown if they are within symbol size. . . 18

3 Total pressure p above solutions of carbon dioxide (1) + cyclohexanol (3) plotted over the mole fraction x_1 of carbon dioxide at different temperatures. Present experimental data: ○ T = 303.8 K; △ T = 352.9 K; ▽ T = 392 K; experimental data of Chen and Lee [6]: + T = 393.15 K. Total pressure p above solutions of oxygen (2) + cyclohexanol (3) plotted over the mole fraction x_2 of oxygen at different temperatures. Present experimental data: • T = 303.8 K; ▲ T = 352.9 K; — Peng-Robinson EOS [11]. The error bars are not shown when they are within symbol size. 19

4 Influence of the total pressure p on the ratio of solute fugacity in vapor phase and solute liquid phase mole fraction. Carbon dioxide: ○ T = 303.8 K; △ T = 352.9 K; ▽ T = 392 K. Oxygen: • T = 303.8 K; ▲ T = 352.9 K; — straight lines. The error bars of the present data are not shown if they are within symbol size. 20

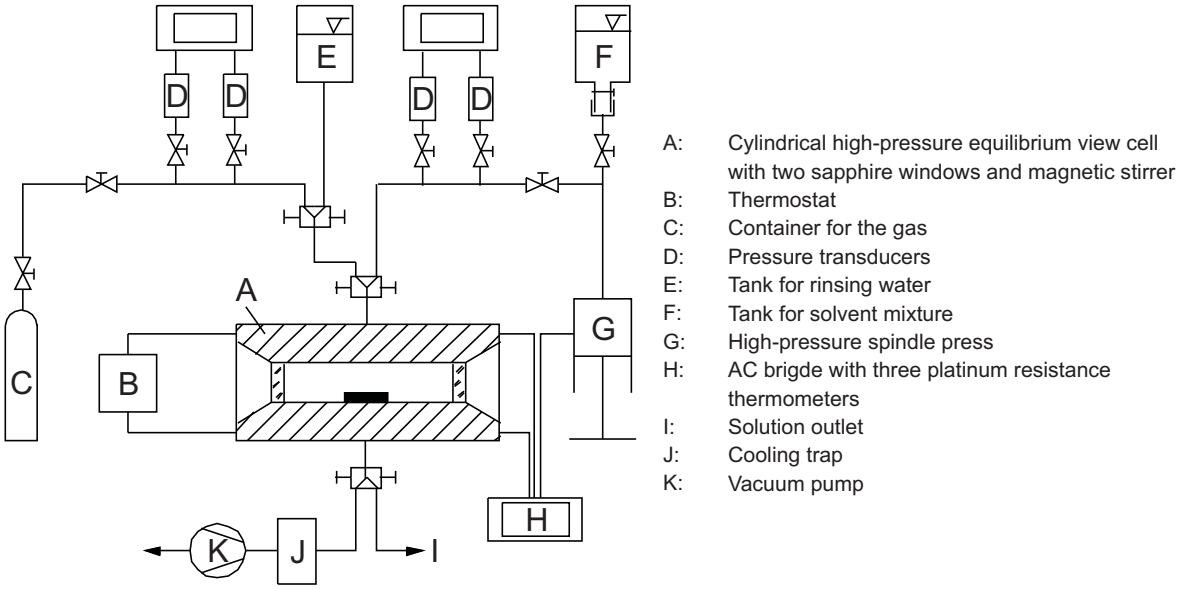

Figure 1: Schematic of the gas solubility apparatus.

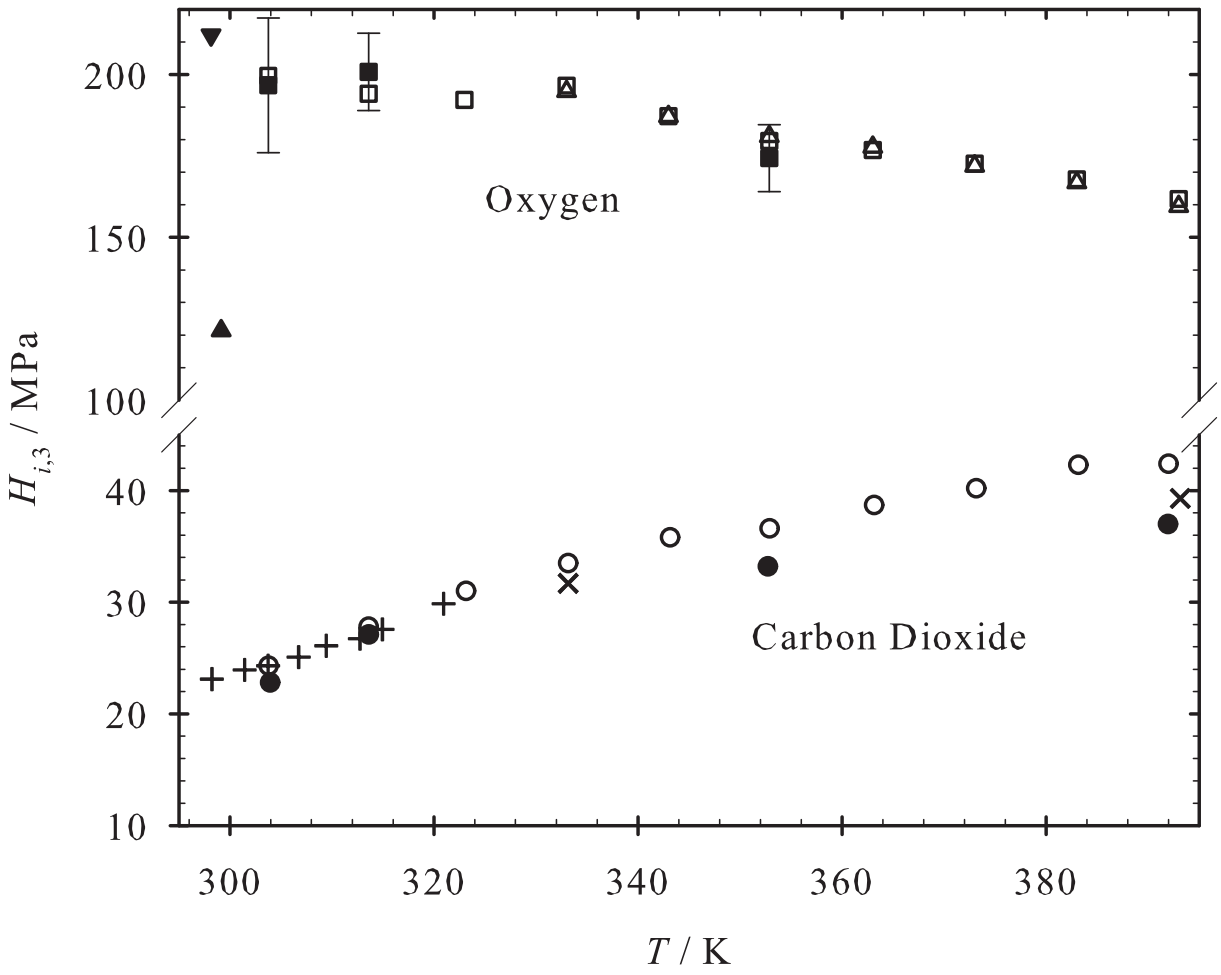

Figure 2: Henry's law constant $H_{1,3}$ of carbon dioxide (1) in cyclohexanol (3): ● present experimental data ; ┼ experimental data by Begley et al [5]; × experimental data by Chen and Lee [6]; ○ present simulation data. Henry's law constant $H_{2,3}$ of oxygen (2) in cyclohexanol (3): ■ present experimental data; ▼ experimental data by Naumenko [10]; ▲ experimental data by Cauquil [9]; □ present simulation data (gradual insertion); △ present simulation data (Widom). The error bars of the present data are not shown if they are within symbol size.

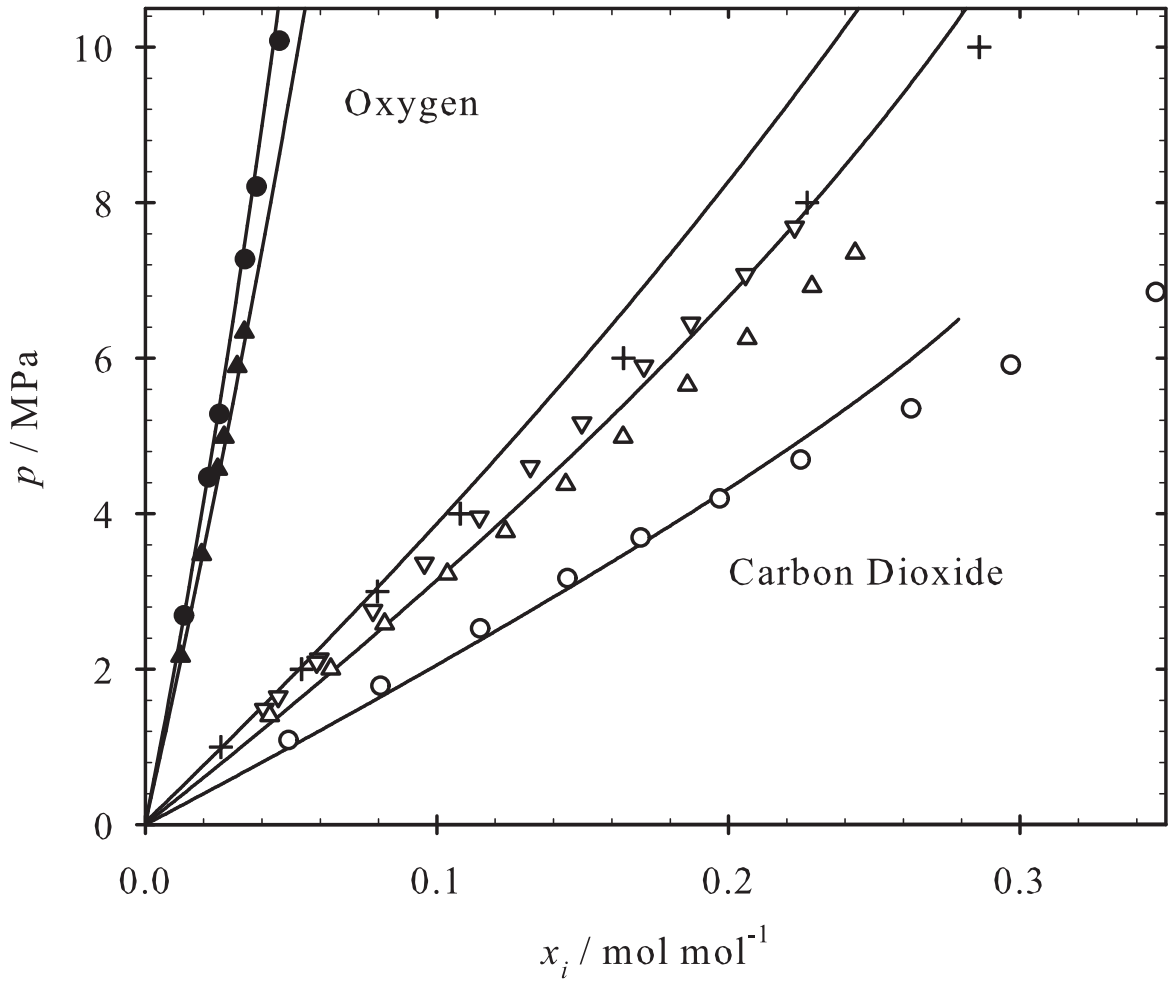

Figure 3: Total pressure p above solutions of carbon dioxide (1) + cyclohexanol (3) plotted over the mole fraction x_1 of carbon dioxide at different temperatures. Present experimental data: ○ $T = 303.8$ K; △ $T = 352.9$ K; ▽ $T = 392$ K; experimental data of Chen and Lee [6]: + $T = 393.15$ K. Total pressure p above solutions of oxygen (2) + cyclohexanol (3) plotted over the mole fraction x_2 of oxygen at different temperatures. Present experimental data: ● $T = 303.8$ K; ▲ $T = 352.9$ K; — Peng-Robinson EOS [11]. The error bars are not shown when they are within symbol size.

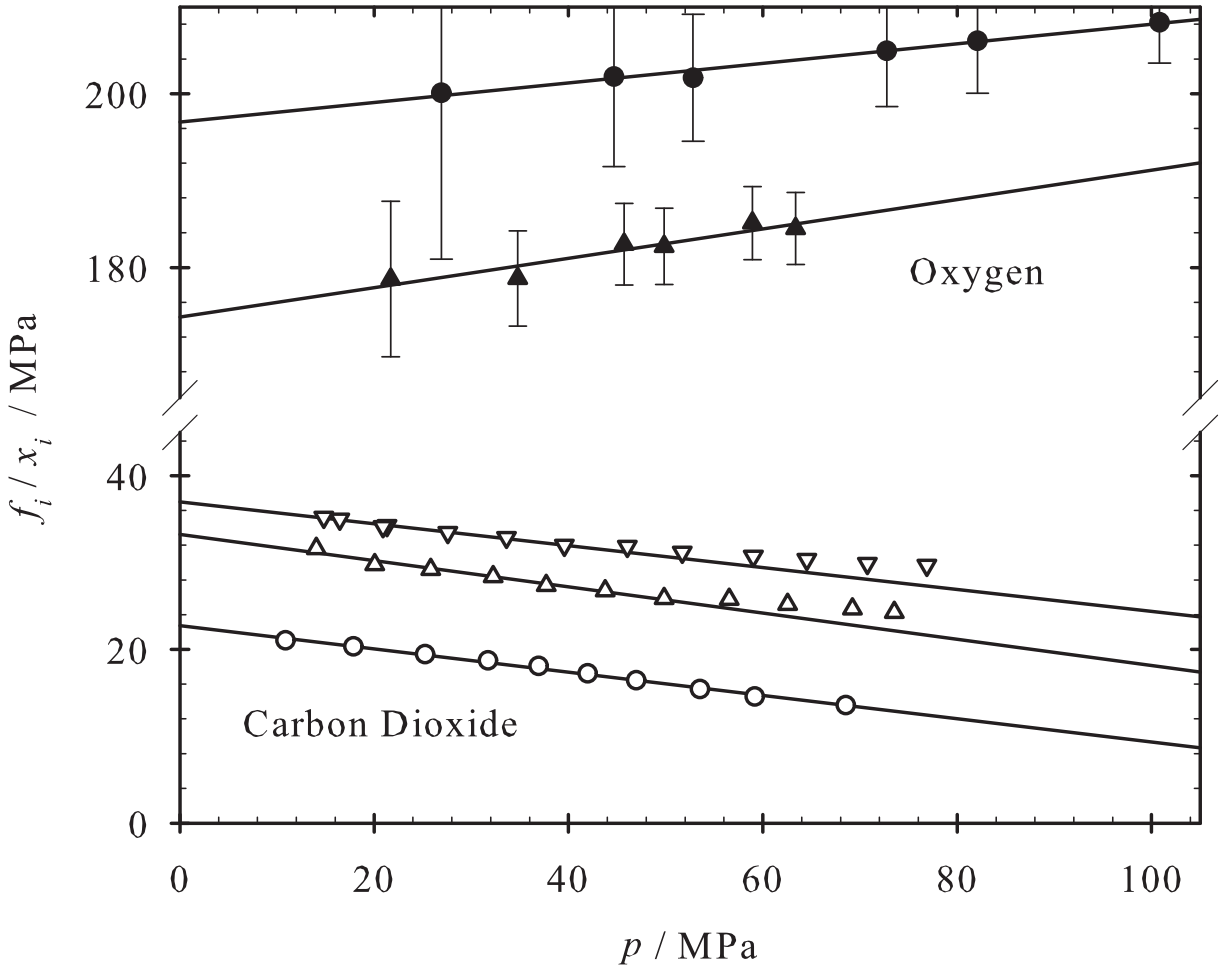

Figure 4: Influence of the total pressure p on the ratio of solute fugacity in vapor phase and solute liquid phase mole fraction. Carbon dioxide: ○ $T = 303.8$ K; △ $T = 352.9$ K; ▽ $T = 392$ K. Oxygen: ● $T = 303.8$ K; ▲ $T = 352.9$ K; — straight lines. The error bars of the present data are not shown if they are within symbol size.